



Contents lists available at ScienceDirect

Journal of King Saud University – Science

journal homepage: [www.sciencedirect.com](http://www.sciencedirect.com)

Original article

# Green synthesized ZnO NPs as effective bacterial inhibitor against isolated MDRs and biofilm producing bacteria isolated from urinary tract infections

Manavalan Murugan<sup>a</sup>, K.R. Beula Rani<sup>b</sup>, J. Albino Wins<sup>c</sup>, Govindan Ramachandran<sup>d</sup>, Feng Guo<sup>e,\*</sup>, Ramzi A. Mothana<sup>f</sup>, Omar M. Noman<sup>f</sup>, Fahd A. Nasr<sup>f</sup>, Muhammad Zubair Siddiqi<sup>g</sup><sup>a</sup> Department of Biomedical Engineering, Noorul Islam Centre for Higher Education, Kumaracoil 629180, Tamil Nadu, India<sup>b</sup> Department of Microbiology, Malankara Catholic College, Mariagiri, Kaliyakkavilai 629153, Kanyakumari District, Tamil Nadu 629180, India<sup>c</sup> Department of Botany, Holy Cross College, Nagercoil 629004, Kanyakumari District, Tamil Nadu, India<sup>d</sup> Marine Pharmacology and Toxicology Laboratory, Department of Marine Science, Bharathidasan University, Tiruchirappalli 620024, Tamil Nadu, India<sup>e</sup> Department of Urology Surgery, Jinan Central Hospital, No. 105, Jiefang Road, Jinan City, Shandong Province 250013, China<sup>f</sup> Department of Pharmacognosy, College of Pharmacy, King Saud University, Riyadh, 11451, Saudi Arabia<sup>g</sup> Department of Biotechnology, Hankyong National University, 327 Jungang Road, Gyeonggi-do 17579, South Korea

## ARTICLE INFO

### Article history:

Received 12 October 2021

Revised 21 November 2021

Accepted 23 November 2021

Available online 27 November 2021

### Keywords:

Nanoparticles

Biomedical application

Antibiotic susceptibility

Minimum inhibition concentration

## ABSTRACT

Based on the importance of multi drug resistant and biofilm forming bacterial spread, the current research work aimed on synthesizing the nanoparticles of zinc oxide from the plant parts of *Limonia acidissima*. They were assayed for their antibacterial activities against biofilm forming urinary tract infected pathogens including *Salmonella paratyphi*, *Shigella*, *Streptococcus*, *Staphylococcus* and *Klebsiella pneumonia* which was confirmed by anti-microbial susceptibility test, 24-well polystyrene plate and modified tube test methods. The formulation of nanoparticles was confirmed by UV-Visible spectrophotometry. Fourier transform infrared spectroscopy revealed the formation of biomolecules that has great involvement in stabilizing the zinc oxide. The size as well as the shape with high resolution was confirmed with electron microscopical studies. It is very clear that zinc oxide nanoparticles have great antimicrobial effect because of its inhibition role against tested urinary tract bacteria by various invitro experiments. This provides a positive thinking on novel drug discovery, in which human health can be improved. Hence, this study provides a scientific support to the medicinal uses of zinc oxide nanoparticles for the treatment of microbial infections.

© 2021 The Author(s). Published by Elsevier B.V. on behalf of King Saud University. This is an open access article under the CC BY-NC-ND license (<http://creativecommons.org/licenses/by-nc-nd/4.0/>).

## 1. Introduction

Worldwide, most prevalence infections are urinary tract infection, and it affected >10% peoples every day among the total of 150 million (Abad et al., 2019). Recent years, the most of the physicians reported that the urinary tract infection is the most recognized bacterial infection and the treatment is failure (Soto et al., 2006). In women, it is very complicated infection due to the sud-

den increase of pregnancy diabetics, functional abnormalities, immunocompromised nature and failure of existing drugs (Hashemzadeh et al., 2021; Katongole et al., 2020). More reports are pointed out about urinary tract infection and it account 80% of multi drug resistant behavior (AL-Mahfoodh et al., 2021; Rajivgandhi et al., 2018). Recently, multiple reports are evidenced that bundles of virulence factors are the important specific reasons for developed multi drug resistant in urinary tract infection (Baiou et al., 2021; Govindan et al., 2018). Especially, extended spectrum beta lactamses, quorum sensing and biofilm formation by exopolysaccharide are the more possible reason (Jafarzadeh et al., 2020; Cheng et al., 2015). Among the urinary tract infection, these three virulence factors contributed almost 75% and developed more resistant against existing drugs (El mekes et al., 2020; Chitra et al., 2010). Almost all the beta lactum antibiotics are ineffective or more susceptible to multi a drug resistant bacterium which leads to biofilm formation.

\* Corresponding author at: Department of Urology Surgery, Jinan Central Hospital, No. 105, Jiefang Road, Jinan City, Shandong Province 250013, China.

E-mail address: [gf6086@sina.com](mailto:gf6086@sina.com) (F. Guo).

Peer review under responsibility of King Saud University.



Production and hosting by Elsevier

Biofilm is an infection caused by bundled pathogenic bacteria contacted each other for produce recurrent infection, especially in urinary tract infections (Hatt and Rather, 2008; Jenke-Kodama et al., 2008). Quorum sensing mediated communication, exopolysaccharide, other external swarming behavior, and some internal cellular parts are the major factors for biofilm production (Delcaru et al., 2016; Arulanandraj et al., 2018). Compare with multi drug resistant bacteria, biofilm produced bacteria having multiple of 100 times efficient against existing pathogens. So, there is need in emergence and worldwide, the inhibition effect of successive antibiotics with virulence alteration role (Hancock et al., 2007). So, recent years plant and their phytochemical mediated nanoparticle was alternative drug choice for inhibit the existing drug resistant pathogens (Li et al., 2018; Liu et al., 2009).

*L. acidissima* is a deciduous tree with slender light branchlets that droops at the tip (Datta et al., 2017; Hartmann et al., 2007). The fruits are spherical with 5–12.5-cm diameter in size. It possesses woody hard outer shell, known as rind (Lavenus et al., 2010; Vidhya and Narain, 2011). The fruit has better effect towards liver and cardiac tonic and also work against diarrhea and dysentery, cough, sore throat etc. The pulp possess various therapeutic effects like anti-inflammatory (Pradhan et al., 2012), antipyretic (Rishton et al., 2008), hypoglycemic (Saadeh and Vyas et al., 2014), antitumorous (Sahoo et al., 2010), antimicrobial (Sahu et al., 2013) and hepato effects (Schmidt et al., 2008; Vidhya and Narain, 2011). The juice of the leaves act as a potent releiver for biliousness and stomach obstacles (Sevinç et al., 2010; Vasant and Narasimhacharyaa, 2011).

Zinc oxide nanoparticle is one of the most research oriented material with multiple focus in downstream applications (Araujo-Lima et al., 2017; Azam et al., 2012). The microcrystals of this nanoparticles are the potent absorbers of UV A and UV B because of its wide region bandgap (Jones et al., 2008). The great rely of zinc oxide on biological evidences mainly focused on size of the particle, time of exposure, effect of concentration parameters, concentration of pH, and strategies of biocompatibility (Kalpana and Devi Rajeswari, 2018; Siddiqi and Husen, 2017). The principle of zinc oxide nanoparticles with effect of light has the tendency of penetrating the bacterial cell wall through diffusion effect (Kumar et al., 2018). The SEM and TEM photography showed that zinc oxide nanoparticles can disintegrate the bacterial cell, penetrate and further accumulate in cytoplasm, and further leads to apoptosis (Chatterjee et al., 1980). It is also considered as multifunctional nanocarriers for the purpose of drug delivering effects. Zinc oxide nanoparticles has considerable array of antimicrobial effects by inhibiting the cell wall and cytoplasm and also the biomolecules (Singh et al., 2017; Li et al., 2018).

In this study, antibacterial activity against selected pathogens is monitored by synthesizing nanoparticles of different plant parts like leaf, bark and shell. The pH of the synthesized nanoparticles is analysed and further structural determination patterns were determined by UV-Visible Spectroscopy, Scanning Electron Microscopy and FTIR analysis. The evaluation strategy of antibacterial activity with synthesized zinc oxide nanoparticles along with MIC was performed. The pathogens selected for antibacterial analysis include *Salmonella paratyphi*, *Shigella*, *Streptococcus*, *Staphylococcus* and *Klebsiella pneumoniae*.

## 2. Materials and methods

### 2.1. Collection and processing of bacteria and plant samples

The multi drug resistant effect of biofilm producing bacteria *Staphylococcus aureus*, *Streptococcus pyogenes* and *Salmonella paratyphi*, *Shigella* sp., *Klebsiella pneumoniae* were obtained from

Department of Marine Science, Bharathidasan University, Tiruchirappalli, Tamil Nadu, India. In addition, the multi-drug resistant behavior and biofilm forming effect was further proved by invitro experiments. The ripe fruits and leaves of *Limonia acidissima* were collected, identified and authenticated by the botanist Dr. C. Jospin Ida from Holy Cross College (Autonomous), Nagercoil, Tamil Nadu, India. Bark, leaves and fruit shell of the plant were collected and used for the study. The samples were dried, chopped and finely powdered and stored in air and light resistant containers. About 20 gms of powdered bark, leaf and fruit shell samples were taken and soaked with 100 ml of sterilised distilled water, boiled at 60 °C for 1 h and finally the extracts were cooled, filtered with Whatman No.1 filter paper, and the filtrate was stored at 4 °C.

### 2.2. Identification of multi drug resistant nature

All the gram positive and gram negative bacteria *Staphylococcus aureus*, *Streptococcus pyogenes* and *Salmonella paratyphi*, *Shigella* sp., *Klebsiella pneumoniae* were performed in invitro experiment for identification of multi drug resistant effect using various antibiotic disc by disc diffusion method including cefotaxime (CTX/30ug), piperacillin (PI/100ug), piperacillin/tazobactam (PIT/100/10), Ceftazidime (CAZ/30 ug), ceftazidime/clavulanic acid (CAC). Briefly, the disc diffusion of this method was followed by Rajivagnndhi et al. (2018), previously done using third generation cephalosporin. Freshly prepared muller hinton agar was swabbed by 48 h culture of *Staphylococcus aureus*, *Streptococcus pyogenes* and *Salmonella paratyphi*, *Shigella* sp., *Klebsiella pneumoniae* without made any droplet of heat and gently put the selected discs on the agar surface. All the plates were monitored under room temperature for 24 h and followed kindly noted the zones around the performed discs containing agar surface places. All the results were compared with standard guidelines of Clinical & Laboratory Standards Institute and interpret the multi drug resistant effect of the tested bacteria.

### 2.3. Discover the biofilm producing efficiency

Based on the multi drug resistant efficiency, the selected bacteria was performed to biofilm detection in 24-well polystyrene well plate method based on the recent reported evidence of Hancock et al., (2007). Clearly, all the chosen bacteria were cultured in freshly prepared sterile nutrient broth with 24 h and 48 h respectively. After 24 h and 48 h time duration, the adherent cells were separated from non-adherent cells of the wells using freshly prepared phosphate buffer solution. In this process, the biofilm forming bacteria could able to absorb the crystal violet because of the virulence production. So, the crystal violet 4% was stained on the wells and discarded after 15–20 min based on the continuous stained formation of bacterial culture. After, for recovering decolonization, initially phosphate buffer solution and alter double distilled water were used 3–4 times respectively. Consecutively, dry the wells using air atmosphere and add 2–3 ml of ethanol for detect the strong biofilm cells by ELIZA reader quantitatively at wave length of 600 nm. Based on the O.D value of the crystal violet observed biofilm positive bacteria was calculated and mentioned as strong or moderate or low biofilm bacteria.

### 2.4. Qualitative analysis of biofilm bacteria

The initial quantitative experiment was later confirmed by qualitative tube test for biofilm confirmation using methodology of recently reported article (Hashemzadeh et al., 2021). Before dis-

carding the culture for crystal violet treatment, all the cultures were taken in a test tube and allowed to grow in tryptic soy broth with 1 day in room atmosphere. After complete mate formation was observed in the edge of the tube, the same freshly prepared crystal violet solution (4%) was treated into the tube after discarding the 24 h culture. Then continuously treated by double distilled water three to four times after phosphate buffer solution wash. Then, dry the tube in clean room temperature and then put in inverted position. Finally, the formed ring in the biofilm tubes were cross checked with previous result and reported as per guidelines of CLSI.

### 2.5. Biosynthesis of zinc oxide nanoparticles

2.97 g of 0.1 M zinc nitrate hexahydrate was taken and added with 400 ml of distilled water. 5 ml of the extract from bark, leaf and shell extracts were added to the corresponding bottles containing 95 ml of zinc nitrate solution, with control. The extracts were incubated at 80 °C for 10 min. Further, the bottles were kept undisturbed up to 72 h for the biosynthesis of nanoparticles. After 72 h of incubation, the bottles were observed for change in colour and pH. UV Visible spectroscopy was done to confirm the interaction between the samples and zinc nitrate solution. Further, centrifugation was done at 5000 rpm for 30 min, pellets were collected and purified.

### 2.6. Characterization of nanoparticles

The powdered zinc oxide nanoparticles were characterized and photographed using Scanning Electron Microscope (SEM). The dried powder was mixed with acetone and loaded in sample holder. The loaded sample was then dried under vacuum and subjected to SEM analysis. The purified dried pellets of control, leaf, bark and shell were subjected to Fourier transform infrared spectroscopy with KBr pellets and spectrum was observed (Resolution-4 nm) under the range of 400–4000/cm.

### 2.7. Biomedical properties of synthesized nanoparticles

#### 2.7.1. Antimicrobial sensitivity test

Muller Hinton agar plates were prepared and the plates were swabbed with all the selected isolates. Using a sterile well cutter, wells were cut on the muller hinton agar plates. The synthesized nanoparticle solution was added along with control antibiotics into the respective wells and incubated for 24–72 h at 37 °C. The zone of inhibitions were measured in mm using standard chart (Mishra et al., 2011).

#### 2.7.2. Minimum inhibitory concentration (MIC)

MIC was performed, to analyse the least concentration of drug that has the effect to inhibit the complete bacterial growth. Add 1.6 ml of nutrient broth in first and last tubes. To all the other tubes add 0.9 ul of nutrient broth. To the first and last tubes, add 10–100 µl of extract and 200 µl of DMSO reagent and mixed well. Serial dilution was performed and the tubes were incubated at 37 °C for overnight. After 24 h, add 20 µl of resazurin dye and incubated at 37 °C for 6–8 h.

#### 2.7.3. Minimum bactericidal concentration (MBC)

The MBC was performed by sub-culturing 100 µl of dilutions from MIC tubes onto Muller-Hinton agar plates. The inoculated plates were incubated for 24 hrs and the highest dilutions with low or no bacterial colony were marked as MBC (Poongodi et al., 2013).

## 3. Results and discussion

### 3.1. Identification of multi drug resistant efficiency in selected bacteria

After measure the zones around the tested discs, the result was suggested and favored to the detected result and all the bacteria were confirmed as multi drug resistant effect. Because, the antibiotic discs of ceftazidime and cefotaxime were produced no zones against almost all the bacteria except *K. pneumoniae* (Fig. 1a). In addition, cefotaxime, piperacillin and piperacillin/tazobactam were produced 8 mm, 12 mm 26 mm zones respectively against *K. pneumoniae* (Fig. 1b). Further, the cross checked evidences against *K. pneumoniae* against the antibiotics of cefotaxime and piperacillin were also shown more similar zones around 8 mm and 12 mm (Fig. 1c). All the results of zones and non-zones measurement were available in Table 1. Based on the clear result, the obtained bacteria were multi drug resistant bacteria and its prevalence was very effective in urinary tract infections. Recently, researchers were reported that the urinary tract infected bacteria shown with more multi drug resistant characteristic nature (Baiou et al., 2021; Jafarzadeh et al., 2020). Similar statement was announced by WHO on 2017, the multi drug resistant bacteria in urinary tract infections were very dangerous, because most of the antibiotics were ineffective (Soto et al., 2006). This statement was agreed by AL-Mahfoodh et al (2021), the urinary tract bacteria were very important bacteria due to the continuous development of multi drug resistant characters against existing antibiotics.

### 3.2. Earlier identification of biofilm formation

Obviously, multi-drug resistant bacteria have the biofilm genes and some virulence factors for production of biofilm (Delcaru et al., 2016). As per the statement, the current result was proved that the obtained urinary bacteria were clearly produced strong biofilm formation. In 24-well plate, initially the complete mate was formed in respective obtained bacteria wells and non-mate formation was shown in universal non-biofilm *K. pneumoniae* MTCC culture. After seen with naked eye with clear mate differentiation of control or treated results were suggested our urinary bacteria as strong biofilm producer. The primary confirmation was later proved by crystal violet observed bacterial colonies and attached cells of the bacteria were exhibited strong biofilm O.D values. One can see, the ELIZA reader results were strongly proposed that the O.D values of >300, >320, >360, >410 and >290 (Fig. 2). According to the CLSI guidelines, the resulted O.D values were meeting out the guidelines and proposed that the selected bacteria were strong biofilm producer (Table 2).

### 3.3. Qualitative analysis of biofilm bacteria

The quantitative result of biofilm formation was finally confirmed by tube ring formation experiment and this study result was more correlated to ring formation. The result was also favor to current study, all the obtained bacteria were shown rigid ring after decolorization with phosphate buffer saline degradation. Contrary, the unstained control was supported to the positive biofilm production (Fig. 3). In addition, the rigid rings were suggested that the bacteria were highly attached on the walls of the tubes. This result was seen after 24–48 h time duration only because of the effect of complete biofilm production virulence factors. In between the time duration of 24–48 h, the virulence factors were highly activated the respective gens for biofilm formation. So, the complete mate was formed by excessive production of exopolysaccharide, proteins and amino acids (Rajivgandhi et al., 2021). In

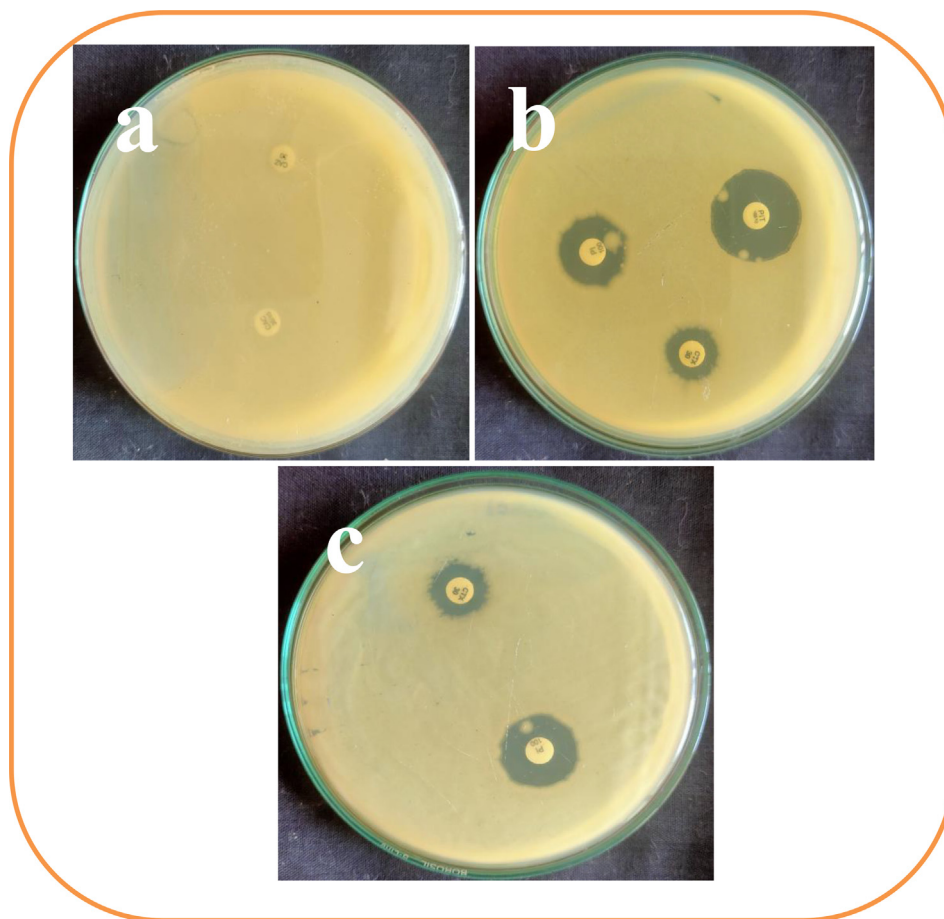


**Fig. 1.** Isolation and identification of multi drug resistant pathogens which isolated from urinary tract infection. The no zone of inhibition (a), little zone of inhibition (b) and cross checking antibiotic (c) against tested *K. pneumoniae* by disc diffusion method.

**Table 1**  
OD values of synthesized ZnO nanoparticle using leaf, bark and shell extracts.

Sl.No.	Wavelength(nm)	Absorption(Å)		
		Leaf	Bark	Shell
1	330	0.5426	0.2197	0.7147
2	340	0.5461	0.1270	0.5449
3	350	0.6155	0.0590	0.3745
4	360	0.6046	0.0315	0.2695
5	370	0.5825	0.0149	0.1754
6	380	0.5581	0.0055	0.0873
7	390	0.5236	0.0005	0.0219
8	400	0.4907	-0.0018	-0.0125

addition, urinary bacteria could be as biofilm positive strains because of the bacterial communication based virulence (Hatt and Rather, 2008). Both the quantitative and qualitative analysis of current study was highly suggested that the obtained bacteria as strong biofilm positive bacteria (Table 3).

### 3.4. Synthesis of ZnO NPs

The reduction of zinc nitrate to zinc oxide when exposed to water extract of *Limonia acidissima* plant parts such as leaf, bark and shell was indicated by the change in colour. The leaf extract exhibit yellow to brown and then to dark brown, bark extract showed light tinch of ash to light yellow and in the case of shell extract, light yellow to moderate yellow. There is no change of colour in the control (Fig. 4).

### 3.5. Characterization of nanoparticles

#### 3.5.1. UV-visible spectroscopy

UV-Visible spectroscopy result was measured, the high peak of 0.6155 Å absorbance was observed for leaf mediated ZnO nanoparticles at 350 nm. 0.2197 Å absorbance was measured for bark mediated ZnO nanoparticles at 330 nm. Another peak was observed in 0.7147 Å for shell mediated ZnO nanoparticles at 330 nm.

#### 3.5.2. FTIR spectrum of zinc oxide nanoparticles

FTIR spectrum of leaf mediated zinc oxide nanoparticles shows mainly 3 absorption band within the 1500 cm<sup>-1</sup>. The absorption bands 3265 cm<sup>-1</sup>, 2113 cm<sup>-1</sup>, 1587 cm<sup>-1</sup> corresponds to various banding. The absorption band 3265 cm<sup>-1</sup> corresponds to strong

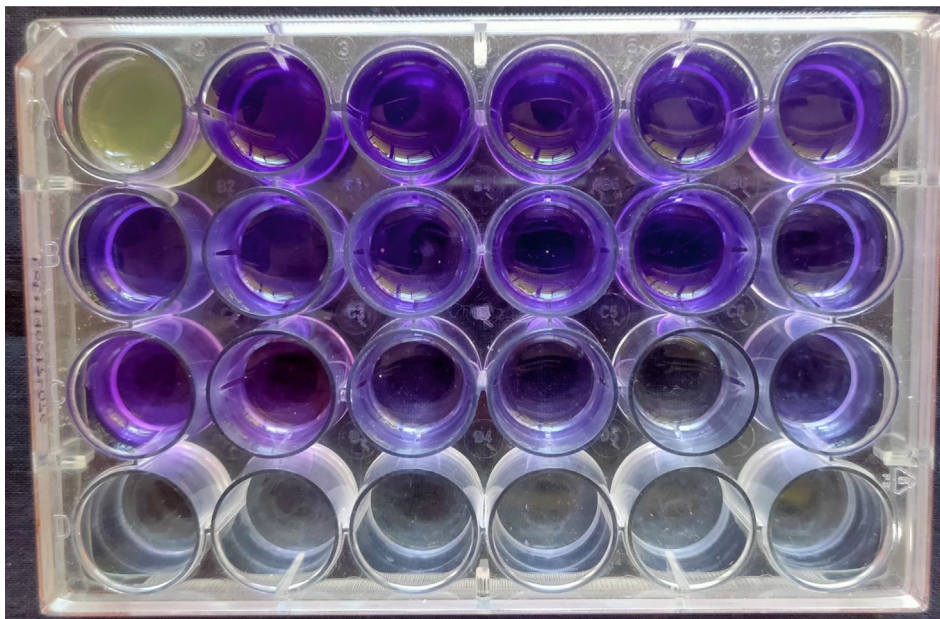


Fig. 2. Biofilm producing bacteria using tissue culture plate method using 24-well plate by ELIZA reader.

Table 2  
Biochemical identification of clinical isolates.

Sl.No.	Biochemical test	Human pathogens				
		<i>Salmonella paratyphi</i>	<i>Shigella</i> sp.	<i>Staphylococcus aureus</i>	<i>Streptococcus pyogenes</i>	<i>Klebsiella pneumoniae</i>
1	Indole	-	+/-	-	-	-
2	MR	+	+	+	-	-
3	VP	-	-	+	-	+
4	Citrate utilization	+	+	+	+	+
5	Urease	-	-	+	-	+
6	TSI	Alk/A	Alk/A	A/A	A/A	A/A
7	H <sub>2</sub> S	+	+	+	+	+
8	Gram staining	-ve rod	- ve rod	+ve cocci	+ve cocci	-ve rod

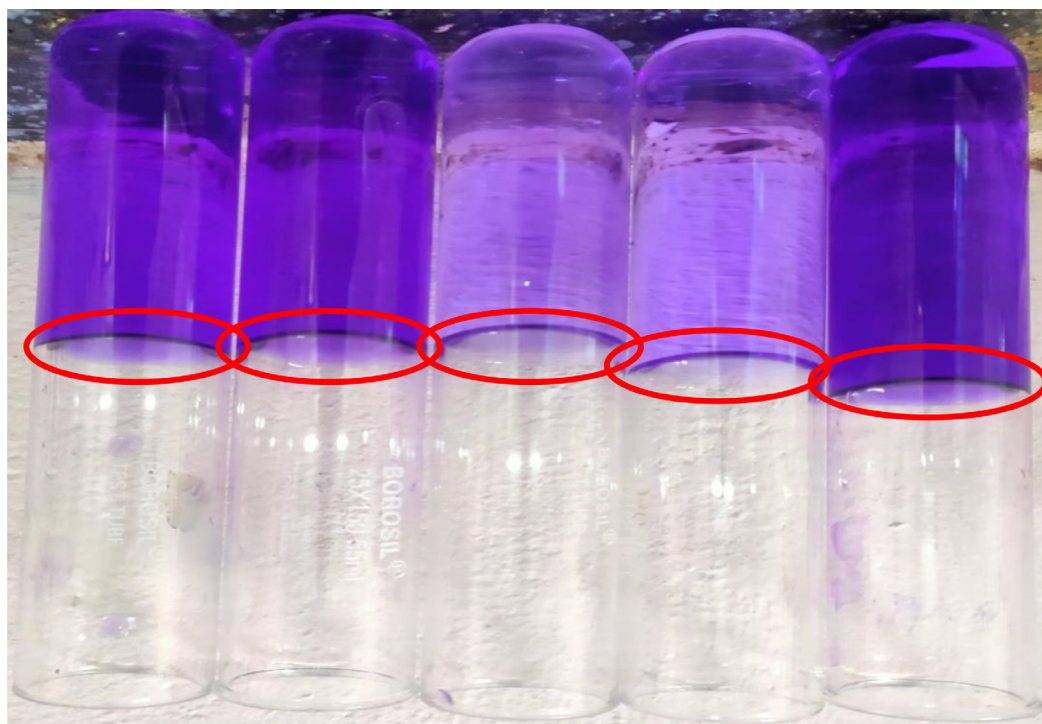


Fig. 3. Biofilm producing bacteria using tissue culture plate method using tube observation (b).

**Table 3**  
Antibacterial effect of synthesized zinc oxide nanoparticles of *Limonia acidissima*.

Sl.No	Microorganism	Zone of inhibition(diameter in mm)		
		Leaf	Bark	Shell
1	<i>Salmonella paratyphi</i>	20 mm	17 mm	17 mm
2	<i>Klebsiella pneumoniae</i>	19 mm	17 mm	15 mm
3	<i>Staphylococcus aureus</i>	16 mm	R	15 mm
4	<i>Streptococcus pyogenes</i>	15 mm	13 mm	16 mm
5	<i>Shigella sp.</i>	14 mm	16 mm	14 mm



**Fig. 4.** Preparation of material for synthesis of ZnO NPs including Plant(*Limonina acidissima*) (a), Bark, leaf and shell extracts of *Limonina acidissima* (b) and Zinc nitrate (control) solution and zinc oxide nanoparticles synthesized from extracts of leaf, bark and shell (c).

broad O—H stretching,  $2113\text{ cm}^{-1}$  leads to weak  $\text{C}\equiv\text{C}$  stretching of alkyne, strong  $\text{N}=\text{C}=\text{S}$  stretching of isothiocyanate and  $1587\text{ cm}^{-1}$  to N—H bending of amine group. The other two absorption bands are  $1405\text{ cm}^{-1}$  and  $1259\text{ cm}^{-1}$ . This  $1405\text{ cm}^{-1}$  band corresponds to O—H bending and strong  $\text{S}=\text{O}$  stretching of sulphate and sulfonylchloride. The absorption peak  $1259\text{ cm}^{-1}$  shows strong C—O stretching of either alkyl aryl ether or aromatic ester.

FTIR spectrum of bark mediated zinc oxide nanoparticles shows 4 absorption band within  $1500\text{ cm}^{-1}$ . The absorption bands are  $3283\text{ cm}^{-1}$ ,  $2926\text{ cm}^{-1}$ ,  $2102\text{ cm}^{-1}$ ,  $1636\text{ cm}^{-1}$ . The absorption band with  $3283\text{ cm}^{-1}$  shows strong sharp  $\text{C}\equiv\text{H}$  stretching of alkyne group. The band with  $2926\text{ cm}^{-1}$  shows medium C—H stretching of alkane. The band with  $2102\text{ cm}^{-1}$  shows strong  $\text{N}=\text{C}=\text{S}$  stretching of isothiocyanate group. The absorption band corresponds to  $1636\text{ cm}^{-1}$  shows strong C=C stretching of monosubstituted alkene. Another band with  $1408\text{ cm}^{-1}$  corresponds O—H bending of alcohol group.

FTIR spectrum of shell mediated zinc oxide nanoparticles shows mainly 3 absorption bands within the range of  $1500\text{ cm}^{-1}$ . They are

$3570\text{ cm}^{-1}$ ,  $3466\text{ cm}^{-1}$ ,  $1636\text{ cm}^{-1}$ . The absorption band  $3570\text{ cm}^{-1}$  corresponds to medium sharp O—H of alcohol group. The absorption with  $3466\text{ cm}^{-1}$  corresponds to strong broad O—H stretching of alcoholic group than the other absorption band  $1636\text{ cm}^{-1}$  corresponds to medium C—C stretching of disubstituted alkane. The other lower absorption bands are  $995\text{ cm}^{-1}$  and  $752\text{ cm}^{-1}$ . The  $995\text{ cm}^{-1}$  leads to strong C=C bend of monosubstituted alcohol and  $752\text{ cm}^{-1}$  corresponds to C=C bending of trisubstituted alkene. All the FTIR figure was available in Fig. 5.

### 3.5.3. Scanning electron microscopy

In SEM analysis, the micrographs of nanoparticles were minute in size with spherical shaped and well distributed in solution. Leaf sample showed clumped spherical particles, whereas bark and shell sample showed different morphology. Bark sample possess nanoparticles of rectangular spike like structures and shell sample shows irregular porous structures. For confirmation of morphology of biosynthesized ZnO NPs were available in Fig. 6.

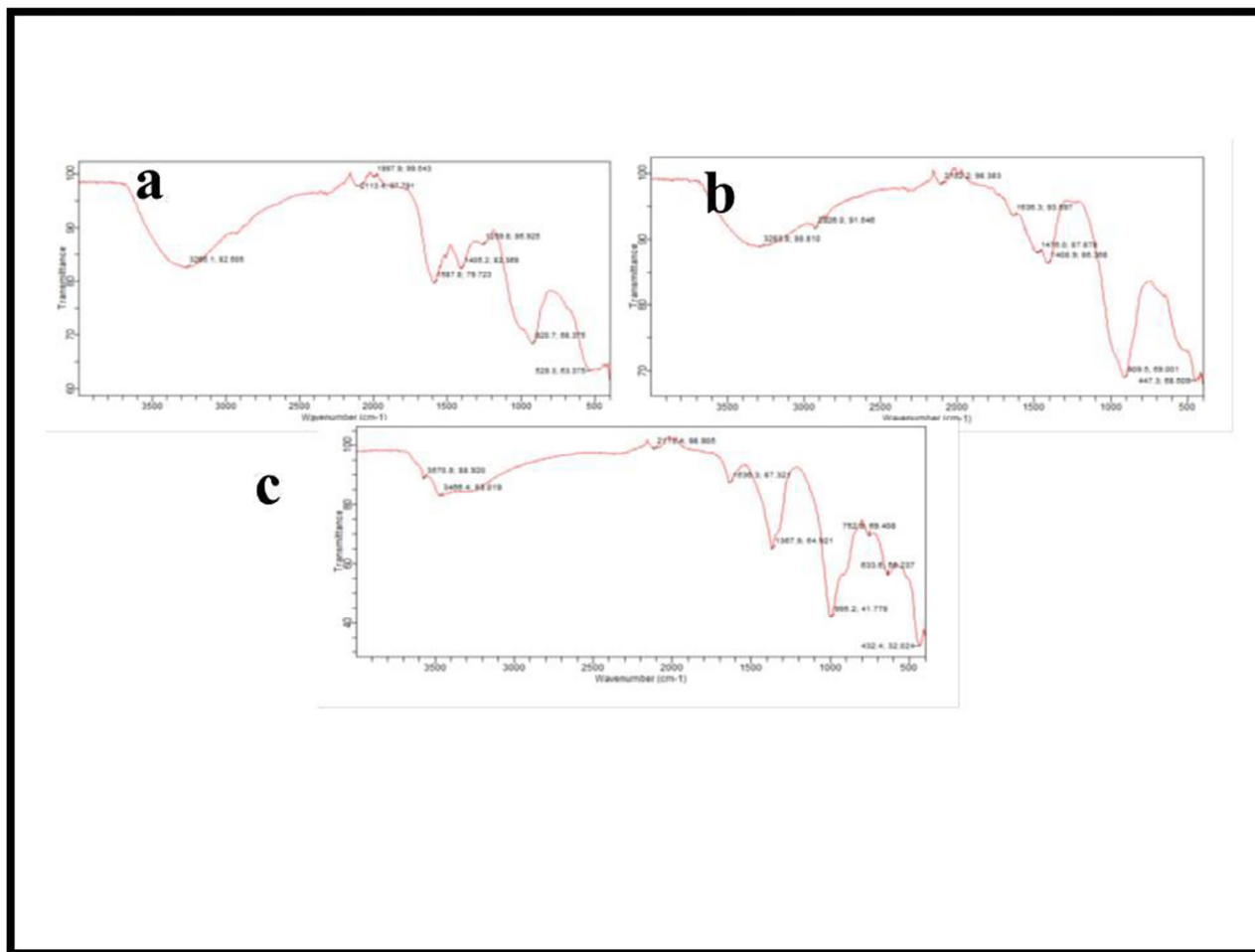


Fig. 5. FTIR analysis of zinc oxide nanoparticles including Leaf (a), bark (b) and Shell (c).

### 3.6. Biomedical properties of ZnO NPs

#### 3.6.1. Antibiotic susceptibility test

The zinc oxide nanoparticles from leaf, bark and shell of *Limonia acidissima* were analyzed for its susceptibility against obtained urinary isolates of *Salmonella paratyphi*, *Shigella* sp., *Staphylococcus aureus*, *Streptococcus pyogenes* and *Klebsiella pneumoniae*. The ZnO nanoparticles from leaf extract of *Limonia acidissima* has potential inhibition against *Salmonella paratyphi* with an inhibition zone of 24 mm, that is followed by *Klebsiella pneumoniae*, *Staphylococcus aureus*, *Streptococcus pyogenes* *Salmonella paratyphi*, and *Shigella* sp. as 22 mm, 20 mm, 26 mm, 18 mm and respectively (Fig. 7). The ZnO nanoparticles of bark extract of *Limonia acidissima* showed a maximum inhibition of zone diameter 17 mm by *Salmonella paratyphi* and *Klebsiella pneumoniae*. This is followed by *Shigella* sp, *Streptococcus pyogenes* with a diameter of 16 mm and 13 mm respectively. *Staphylococcus aureus* shows resistant to the respective nanoparticles (Shermin et al., 2012; Sirelkhathim et al., 2015).

The ZnO nanoparticles of shell extract prevailed a zone of 17 mm by *Salmonella paratyphi*, followed by 16 mm by *Streptococcus pyogenes*, 15 mm by *Staphylococcus aureus* and *Klebsiella pneumoniae* and 14 mm by *Shigella* sp. Comparative study results in a

high degree zone of inhibition seen in ciprofloxacin than streptomycin. The ZnO nanoparticles relates to the inhibitory action of streptomycin. Penicillin G showed no zone of inhibition for all of the selected pathogens.

#### 3.6.2. Minimum inhibitory concentration (MIC)

The bacteria were exposed to different concentrations of zinc oxide nanoparticle; bacterial sensitivity was recorded with increasing concentration of extracts on all the urinary pathogens (Sonawane and Arya et al., 2017; Surmenev et al., 2014). After incubation, the zinc oxide nanoparticles showed blue colour, in the absence of bacteria and pink colour in the presence of bacteria. The minimum inhibitory concentration is 750 µg/mL with 92% inhibition for bark sample, 500 µg/mL with 94% inhibition for leaf and 1000 µg/mL with 88% inhibition for shell extract (Fig. 8a).

#### 3.7. Minimum bactericidal concentration (MBC)

For evidently confirmation, the MIC result was revalidated using MBC experiment and this result was very close to MIC. At the same MIC concentrations, the bacterial growth was very

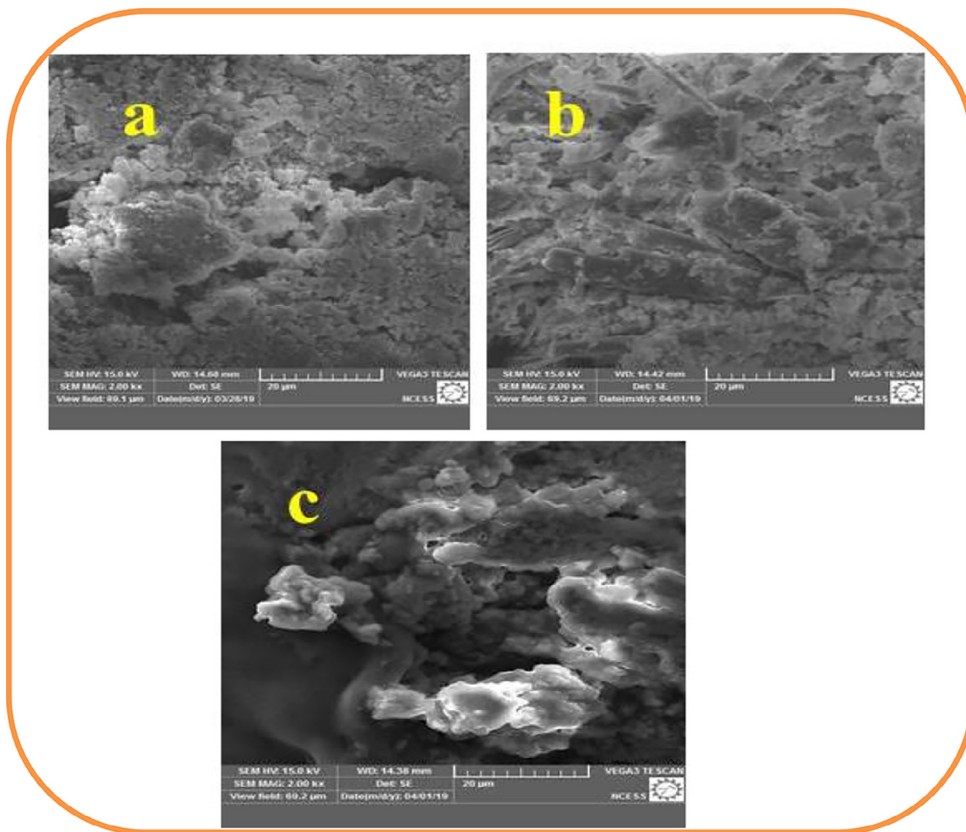


Fig. 6. Scanning Electron Microscopic images for zinc oxide nanoparticles including Leaf (a), bark (b) and Shell (c).

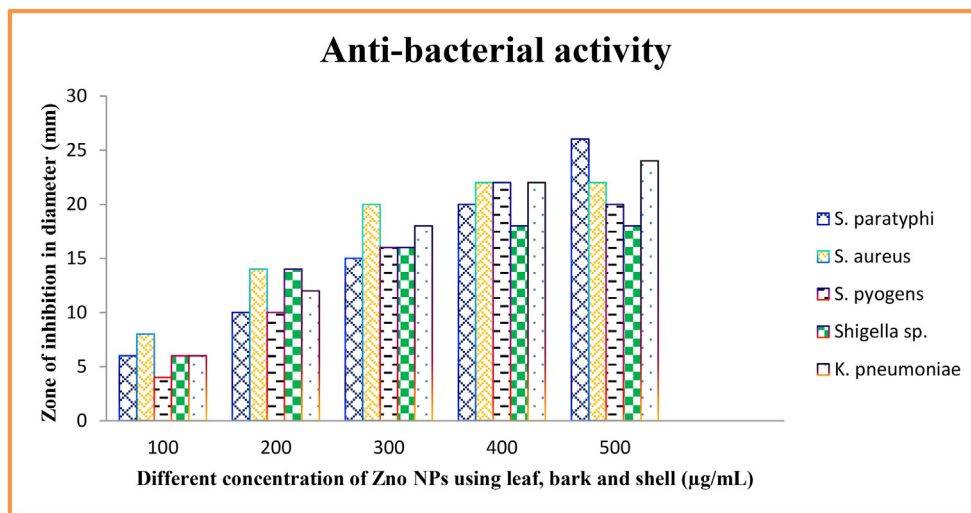
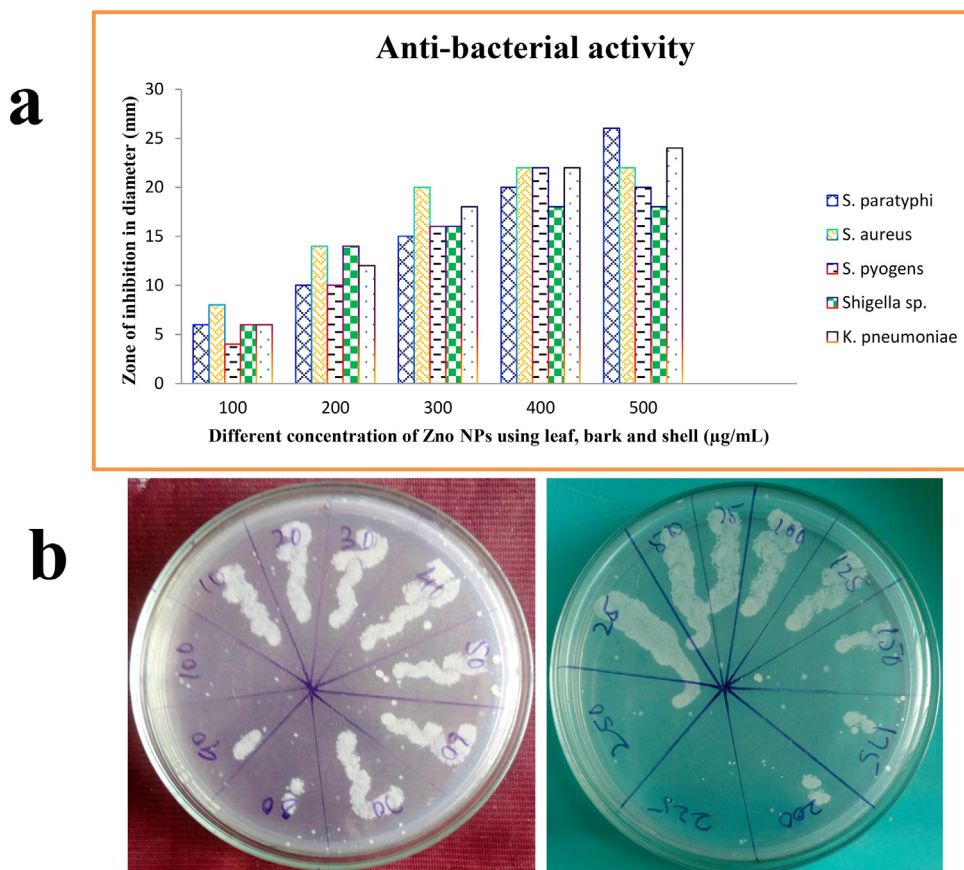


Fig. 7. Antimicrobial activity of ZnO NPs against various pathogens using leaf, bark, and shell by well diffusion method.

low before 100 μg/mL, 80 μg/mL and 250 μg/mL concentrations respectively. At these exact concentrations, the complete bacterial growth was arrested and no growth appeared in muller hinton agar plate (Thomas and Ponnammal et al., 2005; Vijayvergia

and Vijayvergia et al., 2014). In this study of MBC result was more correlate to MIC and suggested that the synthesized ZnO NPs was very efficient against urinary isolates of selected bacteria (Fig. 8b).



**Fig. 8.** Minimum inhibition concentration of leaf, bark, and shell mediated ZnO NPs against *K. pneumoniae* by ELIZA reader (a) and minimum inhibition concentration of ZnO NPs against biofilm producing bacteria *K. pneumoniae* (b).

#### 4. Conclusion

Urinary tract infection is very important in recent years due to the sources for enormous infectious causing factor. So, emerging need to discover new kind of antibiotics that effectively inhibit the biofilm forming pathogens. Based on the seriousness, the formulation and effectiveness of Zinc oxide nanoparticles is eventually considered as a novel and environment friendly technology, as this is promoted as an effective, inexpensive and pollution less product. In the present study, according to the results obtained, the extract preparation of leaves, bark and fruits of *L. acidissima* shall be promptly used for the synthesis of constructive zinc oxide nanoparticles. These specific nanoparticles have specific impact on inhibiting the multi drug resistant biofilm forming microorganisms, which specifically and potentially infected on urinary tract infections. The effective role of zinc oxide nanoparticles shall be promoted as a novel therapeutic agent to overcome various human diseases.

#### Declaration of Competing Interest

The authors declare that they have no known competing financial interests or personal relationships that could have appeared to influence the work reported in this paper.

#### Acknowledgement

The authors extend their appreciation to researchers supporting project number (RSP-2021/119), King Saud University, Riyadh, Saudi Arabia for funding this work.

#### References

- Abad, E.D., Khameneh, A., Vahedi, L., 2019. Identification phenotypic and genotypic characterization of biofilm formation in *Escherichia coli* isolated from urinary tract infections and their antibiotics resistance. BMC Res. Notes 12, 796.
- Soto, S.M., Smithson, A., Horcajada, J.P., Martinez, J.A., Mensa, J.P., Vila, J., 2006. Implication of biofilm formation in the persistence of urinary tract infection caused by uropathogenic *Escherichia coli*. Clin. Microbiol. Infect. 12, 1034–1036.
- Hashemzadeh, M., Dezfuli, A.A.Z., Nashibi, R., Jahangirimehr, F., Akbarian, Z.A., 2021. Study of biofilm formation, structure and antibiotic resistance in *Staphylococcus saprophyticus* strains causing urinary tract infection in women in Ahvaz, Iran. New Microbes New Infect. 39, 100831.
- Katongole, P., Nalubega, F., Florence, N.C., Asiimwe, B., Andia, I., 2020. Biofilm formation, antimicrobial susceptibility and virulence genes of Uropathogenic *Escherichia coli* isolated from clinical isolates in Uganda. BMC Infect. Dis. 20, 453.
- AL-Mahfoodh, W.J.M., Pekacar, F.S., Abbas, A.H., 2021. The molecular study for evaluation the antibiotic resistance of *Escherichia coli* and *Klebsiella pneumoniae* bacteria isolated from urinary tract infection patients, Gene Reports, 25, 101423.
- Govindan, R., Muthuchamy, M., Natesan, M., 2018. Detection of TEM and CTX-M genes from ciprofloxacin resistant *Proteus mirabilis* and *Escherichia coli* isolated on urinary tract infections (UTIs). Microb. Pathog. 121, 123–130.
- Baiou, A., Elbuzidi, A.A., Bakdach, D., Zaqout, A., Alarbi, K.M., Bintaher, A.A., Ali, M.M. B., Elarabi, A.M., Ali, G.A.M., Daghfal, J., Almaslamani, M.A., Ibrahim, A.S.S., Alkhal, A., Omrani, A.S., 2021. Clinical characteristics and risk factors for the isolation of multi-drug-resistant Gram-negative bacteria from critically ill patients with COVID-19. J. Hosp. Infect. 110, 165–171.
- Jafarzadeh, M.M., Moghaddam, M.J.M., Bakhshi, D., 2020. Antimicrobial activity of three plant species against multi-drug resistant *E. coli* causing urinary tract infection. J. Herbal Med. 22, 100352.
- El mekes, A., Zahlane, K., Ait said, L., Tadaloui Ouafi, A., Barakate, M., 2020. The clinical and epidemiological risk factors of infections due to multi-drug resistant bacteria in an adult intensive care unit of University Hospital Center in Marrakesh-Morocco. J. Infect. Public Health 13 (4), 637–643.
- Hatt, J.K., Rather, P.N., 2008. Role of bacterial biofilms in urinary tract infections. Curr. Top. Microbiol. Immunol. 322, 163–192.

- Delcaru, C., Alexandru, I., Podgoreanu, P., Grosu, M., Stavropoulos, E., Chifiriuc, M.C., 2016. Microbial biofilms in urinary tract infections and prostatitis: etiology, pathogenicity, and combating strategies. *Pathogens* 5, 65.
- Hancock, V., Ferrières, L., Klemm, P., 2007. Biofilm formation by asymptomatic and virulent urinary tract infectious *Escherichia coli* strains. *FEMS Microbiol. Lett.* 267, 30–37.
- Arulanandraj, N., S. Dhivya, V. Gopal. A review on herbal nanoparticles. *PharmaTutor* 6.5 (2018): 32–37.
- Lavenus, S., Louarn, G., Layrolle, P., 2010. Nanotechnology and dental implants. *Int. J. Biomater.*, 2010
- Sevinç, A., Berdan, Hanley, Luke, 2010. Antibacterial activity of dental composites containing zinc oxide nanoparticles. *J. Biomed. Mater. Res. B Appl. Biomater.* 94 (1), 22–31.
- Azam, A., Ahmed, A.S., Oves, M., Khan, M.S., Habib, S.S., Memic, A., 2012. Antimicrobial activity of metal oxide nanoparticles against Gram-positive and Gram-negative bacteria: a comparative study. *Int. J. Nanomed.* 7, 6003.
- Rajivgandhi, G.N., Alharbi, N.S., Kadaikunnan, S., Khaled, J.M., Kanisha, C.C., Ramachandran, G., Manoharan, N., Alanzi, K.F., 2021. Identification of carbapenems resistant genes on biofilm forming *K. pneumoniae* from urinary tract infection. *Saudi J. Biol. Sci.* 28 (3), 1750–1756.
- Chatterjee, A., Sarkar, S., Shoolery, J.N., 1980. 7-Phenylacetoxycoumarin from *Limonia crenulata*. *Phytochemistry* 19 (10), 2219–2220.
- Cheng, L., Zhang, K., Weir, M.D., Melo, M.A.S., Zhou, X., Xu, H.H.K., 2015. Nanotechnology strategies for antibacterial and remineralizing composites and adhesives to tackle dental caries. *Nanomedicine* 10 (4), 627–641.
- Chitra, V., Ilango, K., Rajananth, M.G., Soni, D., 2010. Evaluation of *Delonix regia* Linn. flowers for anti-arthritis and antioxidant activity in female wistar rats. *Ann. Biol. Res.* 1 (2), 142–147.
- Datta, A., Patra, C., Bharadwaj, H., Kaur, S., Dimri, N., Khajuria, R., 2017. Green synthesis of zinc oxide nanoparticles using *Parthenium hysterophorus* leaf extract and evaluation of their antibacterial properties. *J. Biotechnol. Biomater.* 07 (03). <https://doi.org/10.4172/2155-952X.1000271>.
- Hartmann, T., 2007. From waste products to ecochemicals: fifty years research of plant secondary metabolism. *Phytochemical*. 68 (22–24), 2831–2846.
- Jenke-Kodama, H., Müller, R., Dittmann, E., 2008. Evolutionary mechanisms underlying secondary metabolite diversity. *Prog. Drug Res.*, 121–140
- Jones, N., Ray, B., Ranjit, K.T., Manna, A.C., 2008 Feb 1. Antibacterial activity of ZnO nanoparticle suspensions on a broad spectrum of microorganisms. *FEMS Microbiol. Lett.* 279 (1), 71–76.
- Kalpna, V.N., Devi Rajeswari, V., 2018. A review on green synthesis, biomedical applications, and toxicity studies of ZnO NPs. *Bioinorg. Chem. Appl.* 2018, 1–12.
- Kumar, A., Deen, B., 2018. Studies on preparation and preservation of squash from wood apple (*Limonia acidissima* L.) fruits. *IJCS* 6 (1), 1513–1516.
- Li, S., Jiang, Q., Liu, S., Zhang, Y., Tian, Y., Song, C., Wang, J., Zou, Y., Anderson, G.J., Han, J.-Y., Chang, Y., Liu, Y., Zhang, C., Chen, L., Zhou, G., Nie, G., Yan, H., Ding, B., Zhao, Y., 2018. A DNA nanorobot functions as a cancer therapeutic in response to a molecular trigger in vivo. *Nat. Biotechnol.* 36 (3), 258–264.
- Liu, Y., He, L., Mustapha, A., Li, H., Hu, Z.Q., Lin, M., 2009. Antibacterial activities of zinc oxide nanoparticles against *Escherichia coli* O157: H7. *J. Appl. Microbiol.* 107 (4), 1193–1201.
- Mishra, A., Garg, G.P., 2011. Antidiabetic activity of fruit pulp of *Feronia elephantum*. *Corr. Pharmacognosy J.* 3 (20), 27–32.
- Poongodi, V.T., K. Punitha, L. Banupriya. 2013. Drying characteristics and quality evaluation of wood apple (*Limonia acidissima*L.) fruit pulp powder. *Int. J. Curr. Trends Res.* 2(1):147–150.
- Pradhan, D., Tripathy, G., Patanaik, S., 2012. Anticancer activity of *Limonia acidissima* Linn (Rutaceae) fruit extracts on human breast cancer cell lines. *Trop. J. Pharm. Res.* 11 (3), 413–419.
- Rishton, G.M., 2008. Natural products as a robust source of new drugs and drug leads: past successes and present day issues. *Am. J. Cardiol.* 101 (10), S43–S49.
- Saadeh, Y., Vyas, D., 2014. Nanorobotic applications in medicine: current proposals and designs. *Am. J. Robotic Surgery* 1 (1), 4–11.
- Sahoo, N., Manchikanti, P., Dey, S., 2010. Herbal drugs: standards and regulation. *Fitoterapia* 81 (6), 462–471.
- Sahu, A.N., 2013. Nanotechnology in herbal medicines and cosmetics. *Int. J. Res. Ayurveda Pharmacy* 4 (3), 472–474.
- Schmidt, B., Ribnicky, D.M., Poulev, A., Logendra, S., Cefalu, W.T., Raskin, I., 2008. A natural history of botanical therapeutics. *Metabolism* 57, S3–S9.
- Shermin, S., Aktar, F., Ahsan, M., Hasan, C.M., 2012. Antioxidant and cytotoxic activity of *Limonia acidissima* L. Dhaka Univ. *J. Pharm. Sci.* 11 (1), 75–77.
- Singh, A., Singh, N.B., Afzal, S., Singh, T., Hussain, I., 2017. Zinc oxide nanoparticles: a review of their biological synthesis, antimicrobial activity, uptake, translocation and biotransformation in plants. *J. Mater. Sci.* 2017.
- Rajivgandhi, G., Maruthupandy, M., Ramachandran, G., Priyanga, M., Manoharan, N., 2018. Detection of ESBL genes from ciprofloxacin resistant Gram negative bacteria isolated from urinary tract infections (UTIs). *Front. Lab. Med.* 2 (1), 5–13.
- Siddiqi, K.S., Husen, A., 2017. Plant response to engineered metal oxide nanoparticles. *Nano Res. Lett.* 12, 92.
- Sirelkhathim, A., Mahmud, S., Seeni, A., Kaus, N.H.M., Ann, L.C., Bakhori, S.K.M., Hasan, H., Mohamad, D., 2015. Review on zinc oxide nanoparticles: antibacterial activity and toxicity mechanism. *Nano-Micro Lett.* 7 (3), 219–242.
- Sonawane, S.K., Arya, S.S., 2017. Bioactive *L. acidissima* protein hydrolysates using Box-Behnken design. *3 Biotech.* 7:218. doi: 10.1007/s13205-017-0862-y. [Crossref], [PubMed], [Google Scholar].
- Surmenev, R.A., Surmeneva, M.A., Ivanova, A.A., 2014. Significance of calcium phosphate coatings for the enhancement of new bone osteogenesis—a review. *Acta Biomater.* 10 (2), 557–579.
- Thomas, A., Ponnammal, N.R., 2005. Preliminary studies on phytochemical and antibacterial activity of *Limonia acidissima* L. plant parts. *Ancient Sci. Life*, 25(2), 57.19–242.
- Vasant, R.A., Narasimhacharyaa, A.V.R.L., 2011. Alleviation of fluoride-induced hepatic and renal oxidative stress in rats by the fruit of *Limonia acidissima*. *Res. Rep. Fluoride* 44 (1), 14–20.
- Vidhya, R., Narain, A., 2011. Development of preserved products using under exploited fruit wood apple (*Limonia acidissima*). *Ame. J. Food Technol.* 6 (4), 279–288.
- Vijayvargia, P., Vijayvergia, R., 2014. A review on *Limonia acidissima* L.: Multipotential medicinal plant. *Int. J. Pharm. Sci. Rev. Res.* 28 (1), 191–195.